

# Quasitwo-dimensional nature of the phonon subsystem of bismuth superconductors

A. A. Bush,<sup>1)</sup> I. N. Goncharuk, Yu. É. Kitaev, M. F. Limonov, Yu. F. Markov, and R. A. Évarestov<sup>2)</sup>

*A. F. Ioffe Physicotechnical Institute, Russian Academy of Sciences*

(Submitted 24 April 1992)

*Zh. Eksp. Teor. Fiz.* **102**, 1587–1605 (November 1992)

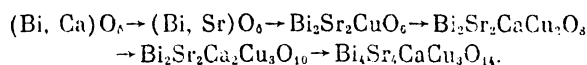
A method for comparative analysis of the vibrational spectra of multicomponent bismuth superconductors was developed and applied to a series of compounds formed as a result of successive addition of new layers;  $(\text{Bi,Ca})\text{O}_\delta \rightarrow (\text{Bi,Sr})\text{O}_\delta \rightarrow \text{Bi}_2\text{Sr}_2\text{CuO}_6 \rightarrow \text{Bi}_2\text{Sr}_2\text{CaCu}_2\text{O}_8 \rightarrow \text{Bi}_2\text{Sr}_2\text{Ca}_2\text{Cu}_3\text{O}_{10} \rightarrow \text{Bi}_4\text{Sr}_4\text{CaCu}_3\text{O}_{14}$ . Zone representations of the space groups were used in a group-theoretic analysis of the symmetry of the normal vibrations of bismuth compounds in the case of both isolated layers and three-dimensional crystals. A symmetry relationship between the layer and bulk (three-dimensional) vibrations was established. The transition from one compound to another was found to result in slight changes in the frequencies of the bulk phonons created by the layer compounds; i.e., these frequencies were governed primarily by the intralayer parameters, indicating that the phonon subsystem in bismuth superconductors was quasitwo-dimensional.

## 1. INTRODUCTION

Phonons participate in the establishment of the high-temperature superconductivity (HTSC), as demonstrated by a whole range of experimental observations (for example, the nonzero isotopic effect), but the role of phonons in the HTSC mechanism has not yet been determined uniquely. Therefore, investigations of phonon subsystems in different high-temperature superconductors is important, particularly in answering the question: which vibrations of what atoms make the contribution to the pairing of carriers in these superconductors?

Numerous investigations have made it possible to provide a fairly reliable interpretation of the vibration spectra of the  $\text{YBa}_2\text{Cu}_3\text{O}_\delta$  (123) system.<sup>1-3</sup> However, in the case of the high-temperature superconducting compounds containing bismuth this situation is somewhat different. There is a wide range of different bismuth high- $T_c$  phases, but the published investigations have been concerned mainly with the compound  $\text{Bi}_2\text{Sr}_2\text{CaCu}_2\text{O}_{8+\delta}$  (2212) for which the Raman scattering spectra are given in many papers.<sup>4-10</sup> The spectra themselves obtained in different investigations agree on the average quite well, but their interpretation is sometimes very different, owing to the multicomponent nature of these compounds and the consequently fairly complex nature of the spectra.

Our aim was a detailed investigation of the phonon subsystem of different bismuth superconductors. To ensure a reliable interpretation of their spectra, we synthesized and investigated a series of compounds formed by successive addition of new layers:



## 2. LAYER STRUCTURE OF BISMUTH SUPERCONDUCTORS

Investigations of the  $\text{Bi}_2\text{O}_3\text{-SrO-CaO-CuO}_{1+\delta}$  system have established that, out of the numerous phases con-

taining Bi, those that exhibit superconducting properties are the compounds forming a homologous series  $\text{Bi}_2\text{Sr}_2\text{Ca}_{n-1}\text{Cu}_n\text{O}_{2n+4+\delta}$  with the phases with  $n = 1, 2,$  and  $3$  known as (2201), (2212), and (2223), respectively,<sup>11,13</sup> as well as their derivatives formed by ordered intergrowth.<sup>14,15</sup> Their compositions and structures resemble those of the Aurivillius phases<sup>16</sup> and they have layer perovskite-like structures complicated by incommensurate modulations and—in the first approximation—are characterized by the tetragonal symmetry ( $I4/mmm$ ) with the fundamental unit cell parameters close to  $a \approx b \approx 5.4 \text{ \AA}$  and  $c \approx 2 \times (9.0 + 3.2n) \text{ \AA}$ .

The layer nature of the bismuth structures and the similar dimensions of their unit cells in the  $xy$  plane favor the formation of composites which consist of separate layers representing the (2201), (2212), and (2223) structures intergrown along the (001) plane. New individual phases form if the intergrowth is ordered. Bearing in mind the possibility of formation of such phases, we can represent the homologous series of bismuth high- $T_c$  compounds by the formula  $\text{Bi}_4(\text{Sr,Ca})_{m+2}\text{Cu}_m\text{O}_\delta$  (Refs. 14 and 15). In this case the number  $m$  represents the number of the  $\text{CuO}_2$  planes in the unit cell with the parameter  $c$  close to  $(18.0 + 3.2m) \text{ \AA}$ . The values  $m = 2, 4,$  and  $6$  correspond to the initial phases (2201), (2212), and (2223), whereas  $m = 3$  corresponds to the recently synthesized composite compound (4413), obtained as a result of ordered intergrowth of the (2201) and (2212) phases.<sup>14,15</sup> The compound  $m = 0$  is close in composition and structure to the copper-free nonsuperconducting variable-composition phase  $\text{Bi}_{1-x}(\text{Sr}_{1-y}\text{Ca}_y)_x\text{O}_{1.5-x/2}$ , where  $0.1 \leq x \leq 0.3$  and  $0 \leq y \leq 1$  ( $\beta$  separate phase), which forms in the  $\text{Bi}_2\text{O}_3\text{-SrO}(\text{CaO})$  system.<sup>17-20</sup> Structures belonging to the homologous series  $\text{Bi}_4(\text{Sr,Ca})_{m+2}\text{Cu}_m\text{O}_\delta$  are shown schematically in Fig. 1.

The common structure elements of all these compounds are double bismuth-oxygen  $2\text{BiO}$  layers (Fig. 1). In the (2201), (2212), and (2223) compounds these layers are separated by perovskite-like blocks containing, respectively,

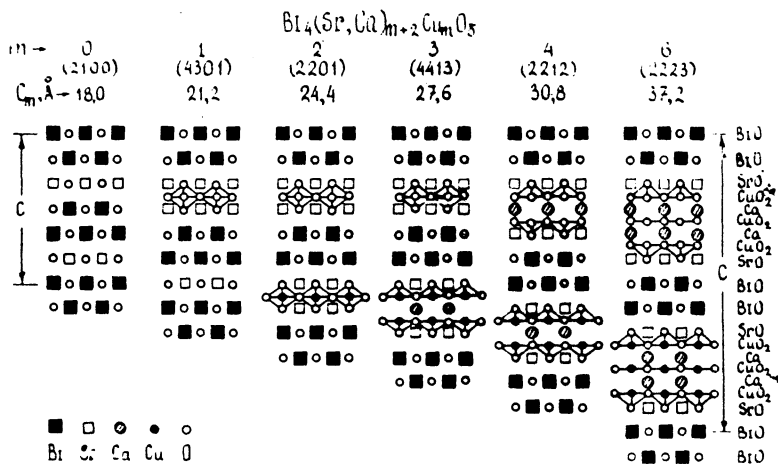


FIG. 1. Schematic representation of the structures of the  $\text{Bi}_4(\text{Sr}, \text{Ca})_{m+2}\text{Cu}_m\text{O}_8$  bismuth series, showing the view of the  $xz$  plane.

the octahedral  $\text{CuO}_6$ , the pyramidal  $\text{CuO}_5$ , and the pyramidal  $\text{CuO}_5$  with square  $\text{CuO}_4$  copper-oxygen polyhedra. All these structures can be represented geometrically by a set of planes, which alternate in a certain sequence along the  $c$  axis: the plane of the Ca atoms, and the  $\text{CuO}_2$ , SrO, and BiO planes.

The structure of  $\text{Bi}_{1-x}(\text{Sr}_{1-y}\text{Ca}_y)_x\text{O}_{1.5-x/2}$  crystals (Fig. 2) consists of "sandwiches" formed by three close-packed planes of BiO, (Bi, Sr, Ca)O, and BiO, which are similar in structure to the superconducting phase layers and which alternate along the  $c$  axis.

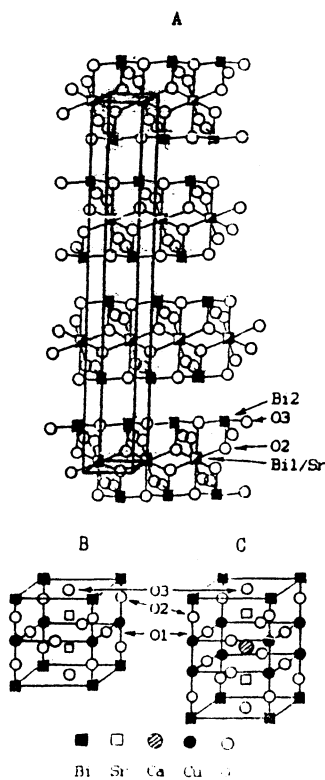


FIG. 2. Crystal structure of the compound  $\text{Bi}_{1-x}\text{Sr}_x\text{O}_{1.5-x/2}$  ( $x = 0.235$ ) according to Ref. 29 (A), and also of the compounds  $\text{Bi}_2\text{Sr}_2\text{CuO}_6$  (B) and  $\text{Bi}_2\text{Sr}_2\text{CaCu}_2\text{O}_8$  (C).

### 3. SYNTHESIS AND CHARACTERIZATION OF SAMPLES. X-RAY STRUCTURE INVESTIGATIONS

We investigated single crystals with the (2212) and (4413) phases separated from ingots recrystallized by zone melting, as well as  $\text{Bi}_{1-x}\text{M}_x\text{O}_{1.5-x/2}$  ( $\beta$ -phase) single crystals grown by the molten solution method, and ceramic samples of the (2201) and (2223) phases (Table I). Single crystals of the (2212) and (4413) compounds were thin platelets with the planes of the bases perpendicular to the  $c$  axis and they exhibited a mica-like cleavage along these planes. The dimensions of the crystals were  $\approx 0.1 \times 2 \times 2$  mm.

Samples of  $\text{Bi}_{1-x}\text{M}_x\text{O}_{1.5-x/2}$  were transparent yellowish-green crystals with a mica-like habit characterized by a very strong cleavage along (001) planes (in the hexagonal setting). The dimensions of these single crystals were  $0.1 \times 6 \times 6$  mm.

The cation chemical composition of these compounds was determined by x-ray spectroscopic microanalysis using a Camebax-301 spectrometer; their crystallographic characteristics were determined by the x-ray powder, rocking, and Weissenberg diffraction methods using a DRON-3 diffractometer and a RGNS-2 x-ray goniometer (Table I).

In the first approximation the symmetry of the Bi superconducting crystals can be regarded as tetragonal. This is indicated by the weakness of the superstructure satellite reflections compared with the main reflections, by the tetragonal pseudosymmetry of the diffraction patterns in the case of the main reflections, and by the near identity (within the limits of the experimental error) of the parameters  $a$  and  $b$  of the fundamental unit cells. A more rigorous analysis of the symmetry of the diffraction patterns based on the main reflections indicates that the fundamental structures are described more accurately by the orthorhombic symmetry. The observed superstructure satellite reflections demonstrate the presence of an incommensurate modulation of the structures along the  $a$  axis. The components of the modulation wave vector  $\mathbf{q}$  along  $a$  and  $b$  axes are practically the same for all the investigated superconducting phases ( $q_x = 0.21a^*$ ,  $q_y = 0$ ); the component  $q_z$  gradually increases from  $0.6c^*$  ( $m = 2$ ) to  $0.80c^*$  ( $m = 3$ ) and  $1.0c^*$  ( $m = 4$  and  $6$ ) on increase in the number of the  $\text{CuO}_2$  planes in the unit cell.<sup>15</sup>

The superconducting properties of the investigated samples were deduced from the experimental temperature

TABLE I. Data on chemical compositions of grown crystals, their symmetry, and dimensions of unit cells.

Phase	Chemical composition	Space group	Unit cell parameters, Å	$T_c$ , K
$\beta$	$\text{Bi}_{0.70}\text{Sr}_{0.30}\text{O}_6$	$D_{3d}^5 (R\bar{3}m)$	$a=3,970(5)$ $c=28,30(5)$	—
$\beta$	$\text{Bi}_{0.78}(\text{Sr}_{0.53}\text{Ca}_{0.47})_{0.22}\text{O}_6$	*	$a=3,933(5)$ $c=28,15(5)$	—
$\beta$	$\text{Bi}_{0.85}\text{Ca}_{0.15}\text{O}_6$	*	$a=3,925(5)$ $c=27,75(2)$	—
(2201)	$\text{Bi}_{2.10}\text{Sr}_{1.90}\text{CuO}_{6+\delta}$	$D_{2h}^{30} (A2ac)$ or $C_{2v}^{13} (A2aa)$	$a=5,376(3)$ $b \approx a$ $c=24,61(2)$	40
(2212)	$\text{Bi}_{2.10}\text{Sr}_{1.72}\text{Ca}_{1.14}\text{Cu}_2\text{O}_{8+\delta}$	*	$a=5,405(5)$ $b \approx a$ $c=30,75(2)$	90
(2223)	$(\text{Bi}_{0.88}\text{Pb}_{0.12})_{2.32}(\text{Sr}_{0.48}\text{Ca}_{0.52})_{3.93}\text{Cu}_3\text{O}_{10+\delta}$	*	$a=5,411(3)$ $b \approx a$ $c=37,07(1)$	108
(4413)	$\text{Bi}_{1.36}\text{Sr}_{3.64}\text{Ca}_{1.10}(\text{Cu}_{0.98}\text{Fe}_{0.02})_3\text{O}_{14+\delta}$	$D_{2h}^{21} (Cmma)$ or $C_{2v}^{15} (Cm2a)$	$a=5,414(5)$ $b \approx a$ $c=27,66(1)$	84

dependences of the magnetic susceptibility, recorded using a RAP-155 vibrating-sample magnetometer, and of the electrical resistivity, measured by the four-probe method. The results of the measurements are given in Table I.

#### 4. ANALYSIS OF THE PHONON SYMMETRY IN THE APPROXIMATION OF AN ISOLATED LAYER

These bismuth structures contain a large number of atoms in the primitive cell, the number of lines in the spectra is large, and the interpretation of these lines is quite difficult. Therefore, a group-theoretic analysis, in which a bulk crystal is considered as a whole (as a three-dimensional system periodic along each dimension), is frequently insufficiently informative.

However, using only symmetry considerations, we can obtain additional information on the vibrational spectra if we bear in mind that the compounds under consideration have a strongly manifested layer structure. Since the intralayer interactions are stronger than those between the layers, it is natural to assume that the whole spectrum of the normal vibrations splits into groups of intralayer vibrations and vibrations of the layers relative to one another. We shall use this approach to analyze first the normal vibrations of a single isolated layer with the symmetry of a two-period three-dimensional (layer) space group<sup>21</sup> and we shall then allow for the influence of the interlayer interaction regarded as a small perturbation. We can then identify normal vibrations created by given layers in the spectrum of a bulk crystal. When the interlayer interaction gives rise to a weak splitting of the intralayer vibrations, we can expect doublets in the spectra.

We shall carry out a group-theoretic analysis of the phonon symmetry in bismuth compounds using the approximation of an isolated layer. The results of this analysis are applicable also to other classes of perovskite-like superconductors: the thallium class  $\text{Tl}_2\text{Ba}_2\text{Ca}_{n-1}\text{Cu}_n\text{O}_{2n+4}$ , the

lanthanum class  $(\text{La,Sr})_2\text{CuO}_4$ , and the yttrium class  $\text{YBa}_2\text{Cu}_3\text{O}_{7-\delta}$ .

We shall consider first the layers formed by copper-oxygen polyhedra of different configurations and consisting of the Cu, O1, and O2 atoms (Figs. 1 and 2) and, second, the 2BiO (2TlO) layers consisting of two bismuth-oxygen (thallium-oxygen) planes. These are the layers that are periodically repeated structure elements giving rise to different perovskite-like compounds.

The bismuth and thallium superconductors contain copper-oxygen layers of three types (Fig. 1): 1) If  $n = 1$ , the structure consists of a layer  $L_1$ , consisting of  $\text{CuO}_6$  octahedra and characterized by the layer symmetry group  $P4/mmm$  ( $DG 61$  in the notation of Ref. 21); 2) if  $n \geq 3$ , there are  $(n - 2)$   $L_2$  layers formed from  $\text{CuO}_4$  squares with the layer symmetry group  $P4/mmm$  ( $DG 61$ ); 3) if  $n \geq 2$ , there are two pyramidal  $\text{CuO}_5$  layers  $L_3$  with the  $P4mm$  ( $DG 55$ ) symmetry. In  $(\text{La,Sr})_2\text{CuO}_4$  compounds there is one  $L_1$  layer whereas in  $\text{YBa}_2\text{Cu}_3\text{O}_{7-\delta}$  there are two  $L_3$  layers. It should be mentioned that a group-theoretic analysis of copper-oxygen layers of the  $L_3$  type was reported in Ref. 22.

The BiO planes have the  $P4/mmm$  ( $DG 61$ ) symmetry. The symmetry of the 2BiO layer is described by the  $DG 64$  ( $P4/n2_1/m2/m$ ) group.

The symmetry of the layer vibrations can be found by the method of zone representations of the space groups.<sup>23,24</sup> Moreover, we shall allow for the fact that the  $DG 55$  layer group is a subgroup of the Fedorov group  $F = C_{4v}^1 (P4mm)$ , the  $DG 61$  group is a subgroup of  $F = D_{4h}^1 (P4/mmm)$ , and the  $DG 64$  group is a subgroup of  $F = D_{4h}^7 (P4/n2_1/m2/m)$ , and we shall allow for the fact that their zone representations are related in a certain manner.<sup>24</sup>

The results of a group-theoretic analysis of the symmetry of the normal vibrations of the investigated layers are given in Tables II–IV for high-symmetry points in the Brillouin zone of the square lattice. Their structure, like the

TABLE II. Phonon symmetry in copper-oxygen ( $L1, L2$ ) layers and in bismuth-oxygen planes.

BiO	$L1$	$L2$	$P4/mmm(DG61)$		$\Gamma$ (00) $D_{4h}$	$M$ $(\frac{1}{2} \frac{1}{2})$ $D_{4h}$	$X$ $(0 \frac{1}{2})$ $D_{2h}$
	1		2	3	4	5	6
Bi	Cu	Cu1	$1a$ (000) $D_{4h}$	$a_{2u}(z)$ $e_u(x, y)$	3- 5-	3- 5-	2- 3-, 4-
O3	-	-	$1c$ $(\frac{1}{2} \frac{1}{2} 0)$ $D_{2h}$	$a_{2u}(z)$ $e_u(x, y)$	3- 5-	2- 5-	3+ 1+, 2+
-	O1	O4	$2f$ $(0 \frac{1}{2} 0)$ $D_{2h}$	$b_{1u}(z)$ $b_{2u}(y)$ $b_{3u}(x)$	3-, 4- 5- 5-	5+ 1+, 2+ 3+, 4+	2-, 3+ 1+, 3- 2+, 4-
-	O2	-	$2g$ (00z) $C_{4v}$	$a_1(z)$ $e(x, y)$	1+, 3- 5+, 5-	1+, 3- 5+, 5-	1+, 2- 3+, 4±

structure of Tables V and VI, is as follows. Column 1 gives the distribution of atoms in the investigated layers (the atoms are numbered in the same way as in bulk crystals—see Fig. 2) in accordance with the Wyckoff positions, labeled using the notation of Ref. 25 and given in column 2 alongside the coordinates of the positions in units of  $a, b$ , and  $c$ , and their local symmetry groups ( $a, b$ , and  $c$  are the fundamental translation vectors for a simple lattice or the translation vectors for the doubled cell in the case of a centered lattice). In column 3 we have the same irreducible representations of the local group which are used to transform the components of the vectors representing the local displacements of the atoms ( $x, y, z$ ). (The notation used for the irreducible representations of the local groups is the same as in Ref. 26.) Columns 4–6 give the indices of the zone representations in the  $k$  basis, obtained by induction from the appropriate irreducible representations of the local group. The indices of zone representations in the  $k$  basis represent sets of indices of the complete irreducible representations of the space group, which can be used to expand the appropriate zone representations and which determine the symmetry of the normal vibrations of a crystal. The numbering of the complete irreducible representations is the same as the numbering in the irreducible

representations of the wave vector groups which are in one-to-one correspondence with the former. It should be noted that the zone representations can be described fully by specifying the sets of the irreducible representations of the wave vector groups only at the high-symmetry points of the Brillouin zone. At the remaining points of this zone the relevant zone representation can be obtained from the compatibility conditions. The symbols for the high-symmetry points in the Brillouin zone, their coordinates in units of  $2\pi/a, 2\pi/b$ , and  $2\pi/c$ , and the corresponding point groups of the wave vector are listed in the headings of columns 4–6; the irreducible representations of the wave vector groups are given in the notation of Ref. 27.

Tables II–VI allow us to obtain the full vibrational representation at the high-symmetry points of the Brillouin zone and, which is particularly important in the interpretation of the vibrational spectra, to establish the displacements of those atoms which contribute to the normal vibrations with a specific symmetry.

For example, the complete vibrational representation of the copper-oxygen layer  $L1$  at the center of the Brillouin zone (i.e., at the point  $\Gamma$ ) has the following form (the atoms listed in parentheses are those which contribute to the given

TABLE III. Phonon symmetry in copper-oxygen ( $L3$ ) layers.

$L3$	$P4mm(DG55)$		$\Gamma$ (00) $C_{4v}$	$M$ $(\frac{1}{2} \frac{1}{2})$ $C_{4v}$	$X$ $(0 \frac{1}{2})$ $C_{2v}$
1	2	3	4	5	6
Cu	$1a$ (00z) $C_{4v}$	$a_1(z)$ $e(x, y)$	1 5	1 5	1 3, 4
O2	$2c$ $(0 \frac{1}{2} z)$ $C_{2v}$	$a_1(z)$ $b_2(y)$ $b_1(x)$	1, 2 5 5	5 1, 2 3, 4	1, 3 1, 4 2, 3

TABLE IV. Phonon symmetry in 2BiO layers.

BiO	$P4/n\ 2_1/m\ 2/m\ (DG\bar{6}4)$	$\Gamma_{(00)}\ D_{4h}$	$M\ (\frac{1}{2}\ \frac{1}{2})\ D_{4h}$	$X\ (0\ \frac{1}{2})\ D_{2h}$	
1	2	3	4	5	6
Bi	$2c$	$a_4(z)$	$1^+, 3^-$	3	1
O3	$(0\ \frac{1}{2}\ z)$ $C_{4v}$	$e(x, y)$	$5^+, 5^-$	1, 2	1, 2

normal vibration; the upper indices of the atoms denote components of the corresponding local displacements and the lower give the Wyckoff positions at which a given atom is located):

$$\Gamma = \Gamma_{opt} + \Gamma_{ac} = \Gamma_1^+ (O2_g^z) + \Gamma_3^+ (O2_g^{xy}) + 3\Gamma_3^- (Cu_a^z; O1_f^z; O2_g^z) + \Gamma_4^- (O1_f^z) + 4\Gamma_5^- (Cu_a^{xy}; O1_f^{xy}; O2_g^{xy}),$$

where  $\Gamma_{ac} = \Gamma_3^- + \Gamma_5^-$ .

It follows therefore that in the case of the  $L\ 1$  layer the complete vibrational representation together with the corresponding selection rules for the vibrations active in the infrared and first-order Raman spectra are as follows (the parentheses give the polarization of light in the case of infrared absorption and the components of the polarizability tensor in the Raman scattering case):

$$A_{1g}(xx, yy, zz) + E_g(xz, yz) + 3A_{2u}(z) + B_{2u} + 4E_u(x, y).$$

Similarly, in the case of the copper–oxygen layer  $L\ 2$ , we have

$$2A_{2u}(z) + B_{2u} + 3E_u(x, y),$$

whereas for the copper–oxygen layer  $L\ 3$ , the corresponding expression is

$$3A_1(z; xx, yy, zz) + B_1(xx, yy) + 4E(x, y; xz, yz),$$

for the BiO plane, we obtain

$$2A_{2u}(z) + 2E_u(x, y)$$

and—finally—the 2BiO layer is described by

$$2A_{1g}(xx, yy, zz) + 2E_g(xz, yz) + 2A_{2u}(z) + 2E_u(x, y).$$

It follows from the above relationships that the  $A_{2u}$  and  $E_y$  vibrations in the BiO plane are active in the Raman scattering. When two BiO planes are united, these vibrations become the  $A_{2u}$  and  $E_u$  vibrations of the 2BiO layers and these are supplemented by intralayer Raman-active vibrations  $A_{1g}$  and  $E_g$ , which represent displacements of the BiO planes relative to one another.

We shall use these results in a complete group-theoretic analysis of bulk bismuth compound crystals.

### 5. GROUP-THEORETIC ANALYSIS OF THE SYMMETRY OF NORMAL VIBRATIONS OF BISMUTH STRUCTURES. RELATIONSHIP BETWEEN LAYER AND BULK VIBRATIONS

#### 5.1. Copper-free structure $Bi_{1-x}(Sr_{1-y}Ca_y)_xO_{1.5-x/2}$

The starting points in the “construction” of the various bismuth semiconductors are copper-free nonsuperconducting  $\beta$ -phase crystals of  $Bi_{1-x}M_xO_{1.5-x/2}$  ( $M = Sr, Ca$ ), as demonstrated in Figs. 1 and 2. The results of an x-ray structure analysis carried out on the crystals investigated by us,

TABLE V. Phonon symmetry of orthorhombic  $Bi_2Sr_2CaCu_2O_8$  crystals.

	$D_{2h}^{20}$	$\Gamma_{(000)}\ D_{2h}$	$Y\ (0\ 1\ 0)\ D_{2h}$	$Z\ (0\ 0\ \frac{1}{2})\ D_{2h}$	$T\ (0\ 1\ \frac{1}{2})\ D_{2h}$	$R\ (\frac{1}{2}\ \frac{1}{2}\ \frac{1}{2})\ C_{2h}$	$S\ (\frac{1}{2}\ \frac{1}{2}\ 0)\ C_{2h}$	
1	2	3	4	5	6	7	8	9
Ca	$2c$	$a_u(z)$	$1^-, 2^-$	$3^+, 4^+$	1	2	$1^+, 2^+$	$1^-, 2^+$
	$(\frac{1\ 1\ 1}{2\ 2\ 2})\ C_{2h}$	$b_u(x, y)$	$3^-, 4^-$	$1^+, 2^+$	2	1	$1^+, 2^+$	$1^+, 2^-$
Bi	$4l$	$a'(x, y)$	$1^+, 2^+, 3^-, 4^-$	$1^+, 2^+, 3^-, 4^-$	1, 2	1, 2	$1^-, 2^\pm$	$1^+, 1^+, 2^-, 2^-$
Sr		$(xy\ \frac{1}{2})\ C_2$	$a''(z)$	$1^-, 2^-, 3^+, 4^+$	$1^-, 2^-, 3^+, 4^+$	1, 2	1, 2	$1^-, 2^\pm$
O2	$C$							
O3								
O1	$4h$	$a(y)$	$1^\pm, 4^\pm$	$1^\pm, 4^\pm$	1, 2	1, 2	$1^\pm, 2^\pm$	$1^\pm, 2^\pm$
O1'	$(0y0)\ C_2$	$b(z, x)$	$2^\pm, 3^\pm$	$2^\pm, 3^\pm$	1, 2	1, 2	$1^\pm, 2^\pm$	$1^\pm, 2^\pm$

Note. The O1 and O1' atoms, belonging to the  $CuO_2$  plane and labeled O1 in the quasitetragonal approximation, become inequivalent in the orthorhombic symmetry.

TABLE VI. Phonon symmetry in  $\text{Bi}_2\text{Sr}_2\text{Ca}_{n-1}\text{Cu}_n\text{O}_{2n+4}$  ( $n = 1, 2, 3$ ) crystals considered in the quasitetragonal approximation.

$n=1$	$n=2$	$n=3$	$D_{4h}^{17}$	$\Gamma$ (000) $D_{4h}$	$M$ (001) $D_{4h}$	$X$ $(\frac{1}{2} \frac{1}{2} 0)$ $D_{2h}$	$P$ $(\frac{1}{2} \frac{1}{2} \frac{1}{2})$ $D_{2d}$	$N$ $(\frac{1}{2} 0 \frac{1}{2})$ $C_{2h}$	
1	2	3	4	5	6	7	8		
Cu	Cu1		1a (000) $D_{4h}$	$a_{2u}(z)$ $e_u(x, y)$	3 <sup>-</sup> 5 <sup>-</sup>	3 <sup>-</sup> 5 <sup>-</sup>	2 <sup>-</sup> 3 <sup>-</sup> , 4 <sup>-</sup>	3 5	2 <sup>-</sup> 1 <sup>-</sup> , 2 <sup>-</sup>
-	Ca	-	1b $(00 \frac{1}{2})$ $D_{4h}$	$a_{2u}(z)$ $e_u(x, y)$	3 <sup>-</sup> 5 <sup>-</sup>	3 <sup>-</sup> 5 <sup>-</sup>	2 <sup>-</sup> 3 <sup>-</sup> , 4 <sup>-</sup>	1 5	1 <sup>+</sup> 1 <sup>+</sup> , 2 <sup>+</sup>
			2c $(0 \frac{1}{2} 0)$ $D_{2h}$	$b_{1u}(z)$ $b_{3u}(x)$ $b_{2u}(y)$	3 <sup>-</sup> , 4 <sup>-</sup> 5 <sup>-</sup> 5 <sup>-</sup>	3 <sup>-</sup> , 4 <sup>-</sup> 5 <sup>-</sup> 5 <sup>-</sup>	3 <sup>+</sup> , 4 <sup>+</sup> 1 <sup>+</sup> , 2 <sup>+</sup> 1 <sup>+</sup> , 2 <sup>+</sup>	5 3, 4 1, 2	1 <sup>+</sup> , 2 <sup>-</sup> 2 <sup>+</sup> , 2 <sup>-</sup> 1 <sup>+</sup> , 1 <sup>-</sup>
Bi Sr O2 O3	Bi Sr O2 O3	Bi Sr O3 Cu Ca	2e (00z) $C_{4v}$	$a_1(z)$ $e(x, y)$	1 <sup>+</sup> , 3 <sup>-</sup> 5 <sup>+</sup> , 5 <sup>-</sup>	1 <sup>+</sup> , 3 <sup>-</sup> 5 <sup>+</sup> , 5 <sup>-</sup>	1 <sup>+</sup> , 2 <sup>-</sup> 3 <sup>±</sup> , 4 <sup>±</sup>	1, 3 5, 5	1 <sup>+</sup> , 2 <sup>-</sup> 1 <sup>±</sup> , 2 <sup>±</sup>
			4g $(0 \frac{1}{2} z)$ $C_{2v}$	$a_1(z)$ $b_1(x)$ $b_2(y)$	1 <sup>+</sup> , 2 <sup>+</sup> , 3 <sup>-</sup> , 4 <sup>-</sup> 5 <sup>+</sup> , 5 <sup>-</sup> 5 <sup>+</sup> , 5 <sup>-</sup>	1 <sup>+</sup> , 2 <sup>+</sup> , 3 <sup>-</sup> , 4 <sup>-</sup> 5 <sup>+</sup> , 5 <sup>-</sup> 5 <sup>+</sup> , 5 <sup>-</sup>	3 <sup>±</sup> , 4 <sup>±</sup> 1 <sup>±</sup> , 2 <sup>±</sup> 1 <sup>±</sup> , 2 <sup>±</sup>	5, 5 1, 2, 3, 4 1, 2, 3, 4	1 <sup>+</sup> , 1 <sup>+</sup> , 2 <sup>-</sup> , 2 <sup>-</sup> 1 <sup>±</sup> , 2 <sup>±</sup> 1 <sup>±</sup> , 2 <sup>±</sup>

and also the results of Ref. 19 indicate that all the  $\beta$ -phase crystals have a symmetry described by the space group  $D_{3d}^5$  ( $R\bar{3}m$ ), corresponding to the rhombohedral system. According to Ref. 18, the  $\text{Bi}_{1-x}\text{Ca}_x\text{O}_8$  system of compounds has the monoclinic symmetry with the space group  $C_{2h}^3$  ( $A2/m$ ). However, in view of the weakness of the monoclinic distortion, we shall use the quasirhombohedral approximation in our group-theoretic analysis.

It follows from the results reported in Ref. 17 for the compounds  $\text{Bi}_{1-x}\text{M}_x\text{O}_{1.5-x/2}$  ( $M = \text{Sr}$ ,  $x = 0.235$ ) that the distribution of atoms in a primitive cell between the symmetry (Wyckoff) positions is as follows: at the position 1a with the coordinates (000) in the hexagonal setting there are Sr and Bi1 atoms (in the proportions of 0.705 Sr and 0.295 Bi), whereas at the 2c positions with the coordinates (00z) and (00 $\bar{z}$ ) there are atoms of Bi2, O2, and O3. A small number (0.148) of the O1 atoms is distributed in the interstices at the general symmetry positions. The total number of the formula units per primitive cell is three.

According to the results of a group-theoretic analysis of the symmetry of the normal vibrations the compounds  $\text{Bi}_{1-x}\text{Sr}_x\text{O}_{1.5-x/2}$  ( $x = 0.235$ ), the complete vibrational representation at the center of the Brillouin zone is:

$$\begin{aligned} \Gamma = & 3\Gamma_1^+( \text{Bi}2_c^z; \text{O}2_c^z; \text{O}3_c^z ) + 3\Gamma_3^+( \text{Bi}2_c^{xy}; \text{O}2_c^{xy}; \text{O}3_c^{xy} ) \\ & + 4\Gamma_2^-( \text{Bi}1/\text{Sr}_a^z; \text{Bi}2_c^z; \text{O}2_c^z; \text{O}3_c^z ) \\ & + 4\Gamma_3^-( \text{Bi}1/\text{Sr}_a^{xy}; \text{Bi}2_c^{xy}; \text{O}2_c^{xy}; \text{O}3_c^{xy} ) \\ = & 3A_{1g}(xx, yy, zz) + 3E_g(xx, yy, xz; xy, yz) + 4A_{2u}(z) \\ & + 4E_u(x, y), \end{aligned}$$

where  $\Gamma_{ac} = A_{2u} + E_u$ .

It follows therefore that in the first-order Raman spectra of  $\text{Bi}_{1-x}\text{M}_x\text{O}_{1.5-x/2}$  the active phonons are those with

the  $A_{1g}$  symmetry in the (xx), (yy), and (zz) scattering geometries, but  $E_g$  in the (xx), (yy), (zz), or (xy) and (yz) scattering geometries.

In the investigated  $\beta$ -phase compounds  $\text{Bi}_{1-x}(\text{Sr}_{1-y}\text{Ca}_y)_x\text{O}_{1.5-x/2}$  at the 1a position there should be atoms of Sr, Ca, and Bi (only the occupancy probabilities change). The occupancy of the 2c positions is not affected by the chemical composition. Therefore, the results of our group-theoretic analysis apply to all the  $\beta$ -phase crystals.

### 5.2. Symmetry analysis of structures of the $\text{Bi}_2\text{Sr}_2\text{Ca}_{n-1}\text{Cu}_n\text{O}_{2n+4}$ ( $n = 1, 2, 3$ ) series

The basis structures of the compounds  $\text{Bi}_2\text{Sr}_2\text{Ca}_{n-1}\text{Cu}_n\text{O}_{2n+4}$  are tetragonal if we ignore the incommensurate modulation, and are orthorhombic if we allow for it. The phonon symmetry at the point  $\Gamma$  of the Brillouin zone of the (2212) crystals was determined in Ref. 8 for the orthorhombic symmetry. The results of the analysis given there, supplemented by our data for the other high-symmetry points in the Brillouin zone are collected in Table V. The phonon symmetry is given in Table VI for all the compounds of the series  $\text{Bi}_2\text{Sr}_2\text{Ca}_{n-1}\text{Cu}_n\text{O}_{2n+4}$  ( $n = 1, 2, 3$ ) considered in the quasitetragonal approximation. The corresponding vibrational representations for the center of the Brillouin zone and the selection rules (applicable in the case of the orthorhombic symmetry and of the quasitetragonal approximation) are given in Table VII. The oxygen atoms are labeled in these tables in the same way as in Fig. 2, namely O1, O2, and O3 belong to the  $\text{CuO}_2$ , SrO, and BiO planes, respectively.

We shall now compare the results of a group-theoretic analysis obtained in the quasitetragonal approximation with the results for an isolated layer (Sec. 4). [The relationship between the normal vibrations and the selection rules for

TABLE VII. Vibrational representations at the center of the Brillouin zone and corresponding selection rules.

Compound	Space groups*	$\Gamma_{\text{opt}} + \Gamma_{\text{ac}}$
$\text{Bi}_{1-x}\text{M}_x\text{O}_6$	$D_{3d}^5$	$3A_{1g}(xx, yy, zz) + 3E_g(xx, yy, zz; xy, yz) + 4A_{2u}(z) + 4E_u(x, y)$
(2201)	$D_{3h}^{17}$	$4A_{1g}(xx, yy, zz) + 4E_g(xz, yz) + 6A_{2u}(z) + B_{2u} + 7E_u(x, y)$
(2212)	$D_{3h}^{17}$	$6A_{1g}(xx, yy, zz) + B_{1g}(xx, yy) + 7E_g(xz, yz) + 7A_{2u}(z) + B_{2u} + 8E_u(x, y)$
(2212)	$D_{2h}^{20}$	$12A_g(xx, yy, zz) + 14B_{1g}(xy) + 7B_{2g}(xz) + 9B_{3g}(yz) + 8A_u + 10B_{1u}(z) + 14B_{2u}(y) + 16B_{3u}(x)$
(2223)	$D_{3h}^{17}$	$7A_{1g}(xx, yy, zz) + B_{1g}(xx, yy) + 8E_g(xz, yz) + 9A_{2u}(z) + 2B_{2u} + 11E_u(x, y)$
(4413)	$D_{3h}^1$	$10A_{1g}(xx, yy, zz) + B_{1g}(xx, yy) + 11E_g(xz, yz) + 13A_{2u}(z) + 2B_{2u} + 15E_u(x, y)$

\*The space groups given here correspond to the approximations employed in the reported study for the various bismuth structures.

Raman-active (2212) crystals of the orthorhombic and quasi-tetragonal symmetries were discussed in Ref. 8.]

The layer vibrational modes in the copper–oxygen layers of the  $L$  1 and  $L$  2 types and the vibrations of the 2BiO layer  $\Gamma_1^+$ ,  $\Gamma_3^-$ ,  $\Gamma_4^-$ ,  $\Gamma_5^+$ , and  $\Gamma_5^-$  are transformed into the bulk modes as follows:

$$\Gamma_1^+ \Rightarrow \Gamma_1^+ + M_1^+, \quad \Gamma_3^- \Rightarrow \Gamma_3^- + M_3^-, \quad \Gamma_4^- \Rightarrow \Gamma_4^- + M_4^-, \\ \Gamma_5^+ \Rightarrow \Gamma_5^+ + M_5^+, \quad \Gamma_5^- \Rightarrow \Gamma_5^- + M_5^-.$$

In the copper–oxygen layers of the  $L$  3 type the intra-layer modes induce the following bulk vibrations<sup>22</sup>

$$\Gamma_1 \Rightarrow \Gamma_1^+ + \Gamma_3^- + M_1^+ + M_3^-; \quad \Gamma_2 \Rightarrow \Gamma_2^+ + \Gamma_4^- + M_2^+ + M_4^-; \\ \Gamma_3 \Rightarrow \Gamma_3^+ + \Gamma_5^- + M_3^+ + M_5^-.$$

It follows from these relationships that the bulk phonons with the symmetry  $\Gamma_1^+$  or  $\Gamma_3^-$  (and also  $\Gamma_2^+$  and  $\Gamma_4^-$ ,  $\Gamma_5^+$  and  $\Gamma_5^-$ ) are induced by the corresponding layer vibrations. Moreover, since the symmetry group of the  $L$  3 layer does not include inversion, the  $\Gamma_1$  and  $\Gamma_5$  layer vibrations are active in infrared absorption and in the first-order Raman scattering. On the other hand, the symmetry group of the crystal as a whole does include inversion and the even components  $\Gamma_1^+$  and  $\Gamma_5^+$  in the corresponding Davydov doublets generated by the layer modes are active only in the Raman scattering, whereas the odd components  $\Gamma_3^-$  and  $\Gamma_5^-$  appear only in infrared absorption. It should also be pointed out that the splitting is governed by the strength of the inter-layer interaction.

It follows therefore that in the case of the (2212) compound the contribution of the copper–oxygen layer  $L$  3 to the total vibrational representation at the center of the Brillouin zone, given in Table VII, is as follows:

$$\Gamma = 3\Gamma_1^+(Cu_e^z, O1_g^z, O2_e^z) + 3\Gamma_3^-(Cu_e^z, O1_g^z, O2_e^z) \\ + \Gamma_2^+(O1_g^z) + \Gamma_4^-(O1_g^z) + 4\Gamma_5^+(Cu_e^{xy}, O1_g^{xy}, O2_e^{xy}) \\ + 4\Gamma_5^-(Cu_e^{xy}, O1_g^{xy}, O2_e^{xy}) \\ = 3A_{1g} + 3A_{2u} + B_{1g} + B_{2u} + 4E_g + 4E_u.$$

Similarly, the contribution of the bismuth–layer 2BiO is

$$\Gamma = 2\Gamma_1^+(Bi_e^z, O3_e^z) + 2\Gamma_3^-(Bi_e^z, O3_e^z) + 2\Gamma_5^+(Bi_e^{xy}, O3_e^{xy}) \\ + 2\Gamma_5^-(Bi_e^{xy}, O3_e^{xy}) = 2A_{1g} + 2A_{2u} + 2E_g + 2E_u.$$

Comparing these contributions with the vibrational representations of the corresponding isolated layers (Sec. 4) we find that in the case of the noncentrosymmetric copper–oxygen layer  $L$  3 the layer modes split into doublets of the bulk vibrations, but in the case of the 2BiO layer there is no such splitting.

### 5.3. Compound $\text{Bi}_4\text{Sr}_4\text{CaCu}_3\text{O}_{14}$

An analysis of the crystal lattice of the (4413) compound carried out using the results of an x-ray structure analysis led us to the conclusion that the symmetry of these crystals considered in the quasitetragonal approximation (ignoring the superstructure) can be described by the space group  $D_{4h}^1$  (simple tetragonal lattice).

It follows from our group-theoretic analysis that the complete vibrational representation at the center of the Brillouin zone is

$$\Gamma = 10A_{1g}(xx, yy, zz) + B_{1g}(xx, yy) + 11E_g(xz, yz) \\ + 13A_{2u}(z) + 2B_{2u} + 15E_u(x, y),$$

where the Raman-active vibrations of the  $A_{1g}$  and  $E_g$  symmetry include contributions of, respectively, the  $z$  and  $x, y$  displacements of the Bi(I, II), Sr(I, II), Cu(II), O1(II), O2(I, II), and O3(I, II) atoms, whereas the contributions to the  $B_{1g}$  vibrations are made by the  $z$  displacements of the O1(II) atom. Here, the numbers I and II label the atoms of the compound (4413) originating from the (2201) and (2212) structures, respectively.

## 6. EXPERIMENTAL INVESTIGATION OF THE RAMAN SCATTERING OF LIGHT

We investigated the optical vibrations of the bismuth compounds by the Raman scattering method. Such scattering was studied employing a Z-24 (Dilor) triple Raman spectrometer and a DFS-24 double spectrometer, using polarized light with wavelengths in the Stokes and anti-Stokes parts of the spectra. The exciting radiation was provided by an Ar laser (made by Spectra-Physics,  $\lambda = 5145 \text{ \AA}$ ,  $P < 50$

TABLE VIII. Frequencies and interpretations of Raman lines.

Compound	Frequencies (cm <sup>-1</sup> ), interpretation, symmetry							
	Bi <i>E<sub>g</sub></i>	Bi <i>A<sub>1g</sub></i>	Sr <i>A<sub>1g</sub></i>	Cu <i>A<sub>1g</sub></i>	O1 <i>B<sub>1g</sub></i>	O1 <i>A<sub>1g</sub></i>	O2 <i>A<sub>1g</sub></i>	O3 <i>A<sub>1g</sub></i>
Bi <sub>0.70</sub> Sr <sub>0.30</sub> O <sub>8</sub>	43	82	-	-	-	-	-	663
Bi <sub>0.85</sub> Ca <sub>0.15</sub> O <sub>8</sub>	44	83	-	-	-	-	-	651
(2201)		80	118	-	-	-	461	629
(2212)		62	118	148	296	395	456	626
(2223)			115		290	406	460	633
(4413)		63	120		295		461	627
YBa <sub>2</sub> Cu <sub>3</sub> O <sub>7</sub>	-	-	120 (Ba)	146	335	435	500	-

mW on the sample) or by an He-Ne laser ( $\lambda = 6328 \text{ \AA}$ ,  $P \approx 5 \text{ mW}$ ). The spectral slit width depended on the signal level and amounted to 6–8 cm<sup>-1</sup> in the case of superconducting samples and 4 cm<sup>-1</sup> in the case of transparent insulating Bi<sub>1-x</sub>M<sub>x</sub>O<sub>1.5-x/2</sub> crystals. The intensities and the frequencies of the individual lines varied somewhat in the spectra obtained for different points on a sample (the frequency was within  $\pm 5 \text{ cm}^{-1}$ ), which could be due to the slight fluctuations of the composition. The values of the Raman scattering frequencies of the investigated compounds are listed in Table VIII.

6.1. Raman scattering of light in Bi<sub>1-x</sub>(Sr<sub>1-y</sub>Ca<sub>y</sub>)<sub>x</sub>O<sub>1.5-x/2</sub> crystals

The spectra of Bi<sub>1-x</sub>(Sr<sub>1-y</sub>Ca<sub>y</sub>)<sub>x</sub>O<sub>1.5-x/2</sub> single crystals shown in Fig. 3 will now be analyzed. Two *lf* lines are hardly shifted when Sr is replaced with Ca, and their frequencies are 43–44 cm<sup>-1</sup> and 82–83 cm<sup>-1</sup>, respectively. The lowest-frequency line appears mainly in the *xy* and *xz* polarizations, and the second (strongest in the Raman spectrum) line is observed in the *xx* and *yy* polarizations, and most clearly for *zz*. Allowing for the independence of the frequencies of these lines of the ratio of the Sr and Ca concen-

trations, and taking into account their polarization properties as well as the prediction of the selection rules (Sec. 5.1) that precisely two different vibrations—usually those of the heaviest atoms in the structure, which are the bismuth atoms (located at the Bi2 position)—are allowed in the Raman spectra, we can identify these lines unambiguously as due to vibrations involving the Bi2 atoms and characterized by the symmetries *E<sub>g</sub>* and *A<sub>1g</sub>*, respectively.

In the hf part of the Raman spectra of Bi<sub>1-x</sub>M<sub>x</sub>O<sub>1.5-x/2</sub> the strongest line is at 650–660 cm<sup>-1</sup>. Its maximum intensity is in the *zz* polarization, characterized by the *A<sub>1g</sub>* symmetry due to vibrations of the light oxygen atoms. It is worth noting that a similar strong *zz*-polarized line at 625–650 cm<sup>-1</sup> is present in the Raman spectra of all the investigated bismuth compounds, but not in the spectra of other superconductors (based on La, Y, or Tl). Therefore, it should be due to the vibrations of the O3 oxygen atoms belonging to the BiO layers, which represent the only shared structure element of these bismuth compounds (Figs. 1 and 2).

On the other hand, another hf line at  $\approx 550 \text{ cm}^{-1}$ , typical of the Raman spectra of Bi<sub>1-x</sub>M<sub>x</sub>O<sub>1.5-x/2</sub>, is not observed in the spectra of bismuth superconductors. Bearing in mind that layers of the (Bi, M)O type with the (Bi1, M) and O atoms displaced relative to one another along the *z* axis are absent from the crystal lattices of Cu-bearing bismuth superconductors (Fig. 2), we must attribute this line to vibrations of the *E<sub>g</sub>* symmetry and involving the oxygen atoms belonging to the (Bi1, M) planes.

In the middle of the intermediate-frequency part of the spectrum (200–500 cm<sup>-1</sup>) there are no strong lines in the Raman spectra of all the investigated Bi<sub>1-x</sub>M<sub>x</sub>O<sub>1.5-x/2</sub> compounds. We shall use this observation in an analysis of the Raman spectra of bismuth superconductors.

6.2. Interpretation of the Raman spectra of the Bi<sub>2</sub>Sr<sub>2</sub>Ca<sub>n-1</sub>Cu<sub>n</sub>O<sub>2n+4</sub> system: allowance for the layer structure of the crystal lattice

Figure 4 shows the Raman spectra of a number of bismuth compounds arranged in the increasing order of the number of layers: these are the spectra of Bi<sub>0.85</sub>Ca<sub>0.15</sub>O<sub>8</sub> crystals, ceramic samples of the (2201) compounds, and (2212) crystals. We shall analyze these spectra in the following self-evident sequence: Raman-active (2201) compounds will be interpreted allowing for the results obtained for the Bi<sub>1-x</sub>M<sub>x</sub>O<sub>1.5-x/2</sub> system and we shall then consider the Raman spectra of the (2212) compounds.

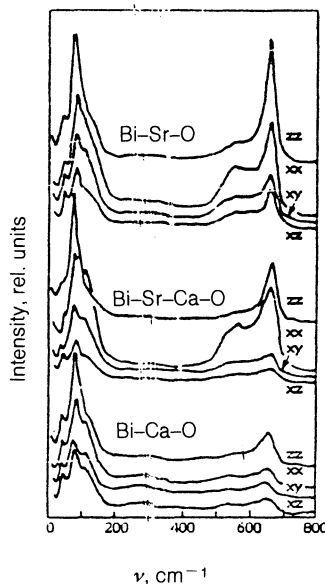


FIG. 3. Raman spectra of Bi<sub>0.70</sub>Sr<sub>0.30</sub>O<sub>8</sub>, Bi<sub>0.78</sub>(Sr<sub>0.53</sub>Ca<sub>0.47</sub>)<sub>0.22</sub>O<sub>8</sub>, and Bi<sub>0.85</sub>Ca<sub>0.15</sub>O<sub>8</sub>, at  $T = 300 \text{ K}$ .



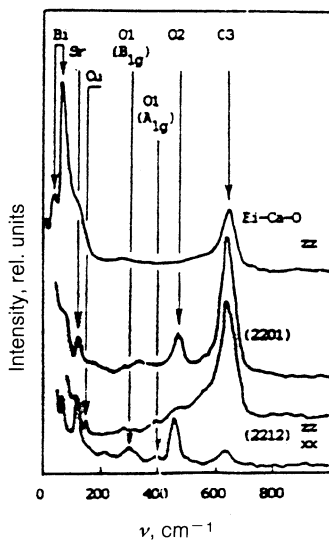


FIG. 4. Raman spectra of  $\text{Bi}_{0.85}\text{Ca}_{0.15}\text{O}_\delta$  crystals in the  $zz$  polarization, and of ceramic samples of the (2201) compounds and of the (2212) crystals in the polarizations  $zz$  and  $xx$ .  $T = 300$  K.

The lines observed in the spectra should be attributed above all to quasitetragonal vibrations (Tables VI and VII). In fact, the orthorhombic splitting is small for Bi superconductors, so that the intensities of the lines (which are additional to the tetragonal and appear because of lowering of the symmetry) are low (after structural phase transitions the intensities of the new lines are proportional to the order parameter, for example, the orthorhombic splitting). In our interpretation we shall rely on the results of our group-theoretic analysis and we shall also allow for the considerable difference between the atomic weights of the elements Bi (209), Sr (88), Cu (64), Ca (40), and O (16).

It follows from the selection rules that the Raman spectra of the (2201) compounds should manifest those vibrations which are active in the case of  $\text{Bi}_{1-x}\text{M}_x\text{O}_{1.5-x/2}$  crystals (i.e., vibrations of the Bi and O3 atoms), as well as the vibrations of Sr and O2 (Tables VI and VII). The vibrations of the atoms belonging to the sole copper-oxygen plane are forbidden in the Raman scattering of light, because these atoms occupy the high-symmetry local positions: Cu is at  $D_{4h}$  and O is at  $D_{2h}$ . By analogy with the already interpreted Raman spectra of  $\text{Bi}_{1-x}\text{M}_x\text{O}_{1.5-x/2}$  crystals, the  $\approx 80$   $\text{cm}^{-1}$  line in the spectra of the (2201) compound should be attributed to the  $A_{1g}$  vibrations of Bi, and the  $629$   $\text{cm}^{-1}$  line should be attributed to the  $A_{1g}$  vibrations of the O3 oxygen belonging to the BiO plane. The second  $I_f$  strong line at  $118$   $\text{cm}^{-1}$  can be attributed naturally to the  $A_{1g}$  vibrations of Sr. Next, bearing in mind that a fairly strong line in the region of  $461$   $\text{cm}^{-1}$  is present in the Raman spectra of all the compounds of the  $\text{Bi}_2\text{Sr}_2\text{Ca}_{n-1}\text{Cu}_n\text{O}_{2n+4}$  series, but is absent from the Raman spectra of  $\text{Bi}_{1-x}\text{M}_x\text{O}_{1.5-x/2}$ , we shall attribute it to the  $A_{1g}$  vibration of the O2 oxygen belonging to the SrO plane.

The next step is the interpretation of the Raman spectra of the (2212) compounds. The (2212) structure is formed from the (2201) structure by the addition of two planes: one of the Ca atoms and the second  $\text{CuO}_2$  plane. Consequently, in accordance with the selection rules, the Raman spectra of

the (2212) compounds differ from those of the (2201) structure by the presence of additionally allowed vibrations of the Cu and O atoms. The vibrations of Ca are inactive in the Raman spectra (local symmetry  $D_{4h}$ ).

Figure 4 shows the Raman spectra of the (2212) crystals in the  $zz$  and  $xx$  polarizations, where the vibrations of the  $A_{1g}$  ( $xx, yy, zz$ ) and  $B_{1g}$  ( $xx, yy$ ) symmetry are active. In the cross polarizations  $xz$  and  $yz$  there are no intense lines. The  $A_{1g}$  symmetry is exhibited by the cophasal vibrations of the Bi, Sr, and Cu atoms and of the oxygen atoms at the O1, O2, and O3 positions (which belong to the  $\text{CuO}_2$ , SrO, and BiO planes, respectively), whereas the  $B_{1g}$  symmetry should be assigned to the contraphasal vibrations of the O1 oxygen. It is clear from Fig. 4 that the additional lines in the Raman spectra of the (2212) system, which are not present in the spectra of (2201), consist of one  $I_f$  line ( $148$   $\text{cm}^{-1}$ ) and two lines in the intermediate part of the spectrum ( $296$  and  $395$   $\text{cm}^{-1}$ ), which should be attributed to the vibrations of the atoms belonging to the  $\text{CuO}_2$  plane. A comparison of the Raman spectra of the  $\text{Bi}_{1-x}\text{M}_x\text{O}_{1.5-x/2}$ , (2201), and (2212) compounds, allowing for the selection rules and for the polarization of the lines in the spectra, makes it possible to propose the following interpretation of the Raman spectra of the (2212) system: the lines representing the vibrations of the heavy atoms are at  $62$   $\text{cm}^{-1}$  (Bi),  $118$   $\text{cm}^{-1}$  (Sr), and  $148$   $\text{cm}^{-1}$  (Cu); the lines due to vibrations of the oxygen atoms are at  $296$   $\text{cm}^{-1}$  (O1 oxygen, vibrational symmetry  $B_{1g}$ ),  $395$   $\text{cm}^{-1}$  (O1, symmetry  $A_{1g}$ ),  $456$   $\text{cm}^{-1}$  (O2,  $A_{1g}$ ),  $626$   $\text{cm}^{-1}$  (O3,  $A_{1g}$ ).

We have thus been able to interpret the majority of the lines in the Raman spectra of the (2212) crystals relating them to the quasitetragonal vibrations of the  $A_{1g}$  and  $B_{1g}$  symmetry. These bulk vibrations are created by the corresponding layer modes (Sec. 5.2) and are responsible for the strongest lines in the Raman spectra. The additional weak lines in these spectra, which can be interpreted using the quasitetragonal approximation ( $281$  and  $321$   $\text{cm}^{-1}$ ), are due to a real lowering of the symmetry to the orthorhombic either by defect or impurity modes.

The Raman spectra of superconducting crystals of the composition  $\text{Bi}_{2.0}\text{Sr}_{1.2}\text{Ca}_{1.0}\text{Cu}_{1.7}\text{O}_\delta$ , which could be regarded as the (2212) structure with a large deficit of the Sr atoms, were reported in Ref. 28. In the  $I_f$  part of the spectra of these crystals there were two strong lines at frequencies  $77$  and  $142$   $\text{cm}^{-1}$ , attributed to the vibrations of the Bi and Cu atoms; i.e., no line which would correspond to the Sr vibrations was found in the region of  $120$   $\text{cm}^{-1}$ . This result was in full agreement with the interpretation of the Raman spectra proposed in the present study.

We shall now consider briefly several differences between the interpretation of the Raman spectra of bismuth superconductors proposed in the present study and those published earlier. For example, according to Refs. 7 and 9 the line in the region of  $\approx 450$   $\text{cm}^{-1}$ , observed in the Raman spectra of the (2212) bismuth compounds, was attributed (by analogy with the Raman spectra of  $\text{YBa}_2\text{Cu}_3\text{O}_\delta$ ) to the vibrations of the O1 atoms, whereas the line at  $\approx 620$   $\text{cm}^{-1}$  was assigned to the O2 vibrations, but we were able to show that the former line was due to the O2 atoms and the latter was due to O3. In Ref. 4, the Raman spectra of the (2212) crystals were investigated in the spectral range  $100$ – $800$

$\text{cm}^{-1}$ , so that the lowest-frequency line associated with the Bi vibrations was ignored. We should mention also that the Raman spectra of the (2212) system reported in Ref. 5 included an additional line in the region of  $\approx 500 \text{ cm}^{-1}$ , which was attributed by the authors of Ref. 5 to vibrations of the oxygen atoms. This line was absent from our spectra and from the Raman spectra reported elsewhere. Its appearance in the spectra given in Ref. 5 could be due to the presence of some impurity phase in the samples.

### 6.3. Raman scattering in the compound $\text{Bi}_2\text{Sr}_2\text{Ca}_2\text{Cu}_3\text{O}_{10}$

In the case of the (2223) structure the Raman spectra include additional, compared with the spectra of the (2212) system, allowed (by the selection rules) vibrations of the Ca atoms which are of the  $A_{1g}$  and  $E_g$  symmetry (Tables VI and VII), which should appear in the lf part of the spectrum. However, the main difference between the spectra lies in the appearance of a new hf line at  $\approx 555 \text{ cm}^{-1}$  (Fig. 5). Its presence in the Raman spectra cannot be explained unambiguously using the quasitragonal approximation. In any case this line is associated with vibrations of the oxygen atoms which may belong either to the main structure (for example, vibrations of the  $E_g$  symmetry) or due to some impurity phase, which is sufficiently homogeneously distributed in a sample. For example, the Raman spectrum of the  $(\text{Ca}_{0.6}\text{Sr}_{0.4})\text{Cu}_{1.75}\text{O}_3$  insulating phase, present together with the bismuth high- $T_c$  compounds, contains one hf line exactly in the region of  $550 \text{ cm}^{-1}$  (Ref. 29).

### 6.4. Raman scattering in the compound $\text{Bi}_4\text{Sr}_4\text{CaCu}_3\text{O}_{14}$

The Raman spectra of the (4413) crystals recorded at room temperature are shown in Fig. 5 and the frequencies of the strongest lines are listed in Table VIII. In these spectra the line frequencies close to those in the Raman spectra of the (2201) and (2212) compounds, and are manifested in the same polarizations, so that the Raman scattering in the (4413) system can be interpreted by analogy with the system,  $\text{Bi}_2\text{Sr}_2\text{Ca}_{n-1}\text{Cu}_n\text{O}_{2n+4}$  ( $n = 1, 2, 3$ ) system. It should be pointed out that the spectra do not exhibit the group-theoretically predicted splitting of the  $A_{1g}$  lines of the vibrations of the Bi, Sr, and O atoms belonging to the (I) and (II) sublattices, which can be explained by the small difference between the frequencies of the corresponding vibrations of the initial (2201) and (2212) structures. Therefore, the number of the experimentally observed lines of the  $A_{1g}$  symmetry is considerably less than the ten lines allowed by the selection rules.

## 7. DISCUSSION OF RESULTS AND CONCLUSIONS

In accordance with the above interpretation of the Raman scattering of light, the strongest lines correspond to the bulk phonons originating from the layer vibrations of the atoms belonging to the copper-oxygen and bismuth-oxygen layers (Sec. 5.2). It is clear from Table VIII that on going from one bismuth compound to another the frequencies of the vibrations of the oxygen atoms belonging to a specific

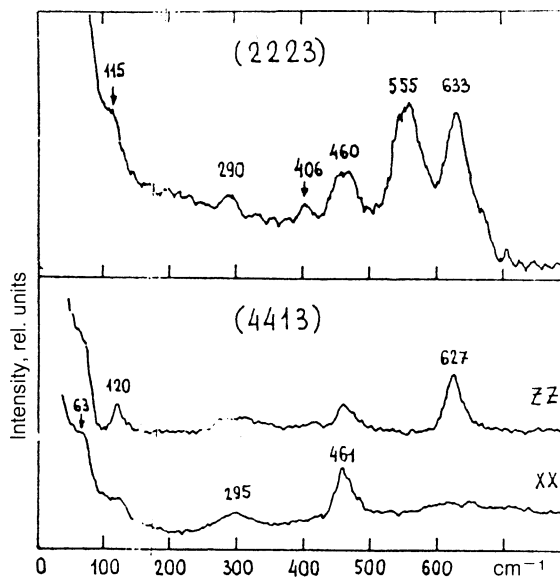


FIG. 5. Raman spectra of the (4413) crystals in the xx and zz polarizations and of the ceramic (2223) samples.  $T = 300 \text{ K}$ .

layer change only slightly; i.e., they are the characteristic frequencies. This applies also to the vibrations of the Bi atoms. Therefore, the values of the frequencies of these vibrations are governed primarily by the intralayer parameters, demonstrating that the phonon subsystem of the investigated bismuth compounds is quasitwo-dimensional. Moreover, in the case of the bismuth and yttrium structure the frequencies of the  $A_{1g}$  and  $B_{1g}$  vibrations of the atoms in analogous layers are also similar (Table VIII), so that we can conclude that this relationship applies also to other perovskite-like superconductors.

The results obtained in the present study demonstrate that the properties of the phonon subsystem of the investigated compounds can be analyzed using an approximate symmetry [i.e., the approximation of an isolated layer, the quasirhombohedral approximation for the  $\text{Bi}_{1-x}(\text{Sr}_{1-y}\text{Ca}_y)_x\text{O}_{1.5-x/2}$  structure, and the quasitragonal for the superconducting Bi compounds], followed by a rigorous symmetry description. Since the second step is equivalent to introduction of a small perturbation, it is possible—without going beyond the framework of a pure symmetry problem—to make a number of predictions about the presence of slightly split doublets in the spectrum, on the relative intensities of the allowed spectral lines, etc. Using the results of a group-theoretic analysis based on the approximate description of the symmetry, we have been able to interpret the majority of the sufficiently strong lines in the Raman spectra with investigated compounds.

One of the main conclusions of the symmetry analysis is the prediction that, on going from an isolated layer (which does not have a center of inversion) to a bulk centrosymmetric crystal, we can expect each layer mode to split into two components with similar frequencies, one of which is Raman-active and the other is active in the infrared spectra. This applies particularly to the layers consisting of copper-oxygen polyhedra; i.e. it applies to the vibrations of the Cu,

O1, and O2 atoms.

We shall now consider the experimental results. We must point out immediately that there have been very few published infrared-spectroscopy investigations of the phonon spectra of high- $T_c$  compounds, owing to the high conductivity in the basal direction and the correspondingly strong reflection of infrared radiation by these quasimetallic objects. Nevertheless, the following frequencies of the infrared-active vibrations of the oxygen atoms in  $\text{Bi}_2\text{Sr}_2\text{CaCu}_2\text{O}_8$  crystals (when the polarization is  $E \parallel z$ ) are given in Ref. 30:  $\nu_{T1} = 445 \text{ cm}^{-1}$ ,  $\nu_{L1} = 465 \text{ cm}^{-1}$ ,  $\nu_{T2} = 594 \text{ cm}^{-1}$ , and  $\nu_{L2} = 614 \text{ cm}^{-1}$ . We can see that these values are close to the frequencies of the Raman-active vibrations of the O2 and O3 atoms, which are 456 and 626  $\text{cm}^{-1}$ . Similar pairs of vibrations can be identified also in the spectra of thallium superconductors. According to Ref. 31, the Raman spectrum of  $\text{TiBa}_2\text{CaCu}_2\text{O}_7$  includes lines with frequencies 116, 146, 403, and 520  $\text{cm}^{-1}$ , whereas the Raman spectrum of  $\text{Tl}_2\text{Ba}_2\text{CaCu}_2\text{O}_8$  includes lines at frequencies 109, 132, 158, 410, 495, and 602  $\text{cm}^{-1}$ . The infrared spectra of  $\text{Tl}_{0.65}\text{Pb}_{0.45}\text{Ba}_2\text{CaCu}_2\text{O}_7$  include lines due to vibrations at frequencies 165, 230, 290, 490, and 580  $\text{cm}^{-1}$  (Ref. 32). It should be mentioned also that the spectra of  $\text{YBa}_2\text{Cu}_3\text{O}_7$  recorded at  $T < T_c$  exhibit anomalous temperature dependences of the line positions: in the Raman spectra this applies to the vibrations of the O1 atoms at the frequency of 335  $\text{cm}^{-1}$  (Ref. 33), whereas in the infrared spectra it applies to the vibrations with frequencies 275 and 315  $\text{cm}^{-1}$  (Ref. 34). Consequently, an examination of the spectra of different high- $T_c$  compounds makes it possible to identify the pairs consisting of the even and odd vibrations with similar frequencies (representing the result of splitting of the layer mode) and similar temperature dependences, which is a direct manifestation of the quasitwo-dimensional nature of the phonon subsystem and confirms the validity of the earlier layer approach to vibrational spectra of bismuth compounds.

We thus investigated various superconducting and non-superconducting bismuth compounds and we carried out a complete group-theoretical analysis of the symmetry of the normal vibrations for isolated layers and three-dimensional crystals. A comparative analysis of the Raman spectra of some of the compounds, differing in respect of the composition and the number of layers, and the use of the results of a group-theoretic analysis, made it possible to identify the lines corresponding to the totally symmetric vibrations of all the atoms occurring in these compounds. It was thus established that transition from one bismuth compound to another changes only slightly the frequencies of the bulk phonons originating from the corresponding layer modes (these are the characteristic frequencies); i.e., these frequencies are governed primarily by the intralayer parameters, demonstrating the quasitwo-dimensional nature of the phonon subsystem in bismuth superconductors.

The authors are grateful to A. A. Kaplyanskiĭ and A. G. Panfilov for discussing the results and critical comments.

- <sup>1)</sup> Moscow Institute of Radio Engineering, Electronics, and Automation.  
<sup>2)</sup> St. Petersburg University.

- <sup>1</sup> R. Liu, C. Thomsen, W. Kress *et al.*, Phys. Rev. B **37**, 7971 (1988).  
<sup>2</sup> V. D. Kulakovskii, O. V. Misochko, and V. B. Timofeev, Fiz. Tverd. Tela (Leningrad) **31**(9), 220 (1989) [Sov. Phys. Solid State **31**, 1599 (1989)].  
<sup>3</sup> M. F. Limonov, Yu. F. Markov, A. G. Panfilov *et al.*, Physica (Utrecht) **C 191**, 255 (1992).  
<sup>4</sup> M. Cardona, C. Thomsen, R. Liu *et al.*, Solid State Commun. **66**, 1225 (1988).  
<sup>5</sup> L. A. Farrow, L. H. Greene, J. M. Tarascon *et al.*, Phys. Rev. B **38**, 752 (1988).  
<sup>6</sup> M. Stavola, D. M. Krol, L. F. Schneemeyer *et al.*, Phys. Rev. B **38**, 5110 (1988).  
<sup>7</sup> O. V. Kosogov, M. V. Belousov, V. A. Vasil'ev *et al.*, Pis'ma Zh. Eksp. Teor. Fiz. **48**, 488 (1988) [JETP Lett. **48**, 530 (1988)].  
<sup>8</sup> A. A. Bush and I. V. Gladyshev, Sverkhprovodimost' (KIAE) **2**(9), 104 (1989) [Superconductivity **2**(9), 117 (1989)].  
<sup>9</sup> M. N. Iliev and V. G. Hadjiev, Physica (Utrecht) **C 157**, 495 (1989).  
<sup>10</sup> I. V. Aleksandrov, A. B. Bykov, A. F. Goncharov *et al.*, Pis'ma Zh. Eksp. Teor. Fiz. **49**, 150 (1989) [JETP Lett. **49**, 175 (1989)].  
<sup>11</sup> C. Michel, M. Hervieu, M. M. Borel *et al.*, Zh. Phys. B **68**, 421 (1987).  
<sup>12</sup> B. Reveau, C. Michel, and M. Hervieu, J. Solid State Chem. **88**, 140 (1990).  
<sup>13</sup> A. A. Bush, I. S. Dubenko, C. É. Mrost *et al.*, [Superconductivity **3**, 409 (1990)].  
<sup>14</sup> A. A. Bush, [Superconductivity **3**, 1475 (1990)].  
<sup>15</sup> A. A. Bush, B. N. Romanov, I. V. Isakov *et al.* Sverkhprovodimost' (KIAE) (in press) [Superconductivity (in press)].  
<sup>16</sup> B. Aurivillius, Ark. Kemi **2**, 519 (1950).  
<sup>17</sup> P. Conflant, J.-C. Boivin, and D. Thomas, J. Solid State Chem. **18**, 133 (1976).  
<sup>18</sup> S. K. Blower and C. Greaves, Mater. Res. Bull. **23**, 765 (1988).  
<sup>19</sup> P. Conflant, J.-C. Boivin, and D. Thomas, J. Solid State Chem. **35**, 192 (1980).  
<sup>20</sup> A. A. Bush, Yu. É. Kitaev, M. A. Kulikov *et al.*, Fiz. Tverd. Tela (Leningrad) **34**, 148 (1992) [Sov. Phys. Solid State **34**, 77 (1992)].  
<sup>21</sup> E. A. Wood, Bell System Monograph No. 4680 (1964).  
<sup>22</sup> I. P. Ipatova, Yu. É. Kitaev, V. G. Malyskin, and R. A. Évarestov, Fiz. Tverd. Tela (Leningrad) **32**, 1565 (1990) [Sov. Phys. Solid State **32**, 918 (1990)].  
<sup>23</sup> O. V. Kovalev, *Irreducible Representations of the Space Groups*, Gordon and Breach, New York, (1965).  
<sup>24</sup> R. A. Évarestov and V. P. Smirnov, *Methods of the Group Theory in Quantum Chemistry of Solids* [in Russian], Leningrad State University (1987), p. 375.  
<sup>25</sup> *International Tables for Crystallography* (ed. by T. Hahn), Vol. A. Space-Group Symmetry, D. Reidel, Dordrecht, Netherlands (1983), p. 854.  
<sup>26</sup> C. J. Bradley and A. P. Cracknell, *The Mathematical Theory of Symmetry in Solids: Representation Theory for Point Groups and Space Groups*, Oxford University Press (1972), p. 745.  
<sup>27</sup> S. C. Miller and W. F. Love, *Tables of Irreducible Representations and Co-Representations of Magnetic Space Groups*, Pruett Press, Boulder, CO (1967), p. 1095.  
<sup>28</sup> C. Durčok, M. F. Limonov, Yu. F. Markov *et al.*, Fiz. Tverd. Tela (Leningrad) **31**(7), 282 (1989) [Sov. Phys. Solid State **31**, 1261 (1989)].  
<sup>29</sup> M. N. Iliev and V. G. Hadjiev, Physica (Utrecht) **C 156**, 193 (1988).  
<sup>30</sup> G. Ruani, C. Taliani, R. Zamboni *et al.*, Solid State Commun. **78**, 979 (1991).  
<sup>31</sup> L. V. Gasparov, V. D. Kulakovskii, O. V. Misochko *et al.*, Pis'ma Zh. Eksp. Teor. Fiz. **49**, 58 (1989) [JETP Lett. **49**, 68 (1989)].  
<sup>32</sup> T. Zetterer, M. Franz, J. Schützmann *et al.*, Solid State Commun. **75**, 325 (1990).  
<sup>33</sup> R. M. McFarlane, H. Rosen, and H. Seki, Solid State Commun. **63**, 831 (1987).  
<sup>34</sup> A. Wittlin, R. Liu, M. Cardona *et al.*, Solid State Commun. **64**, 477 (1987).

Translated by A. Tybulewicz